

# Supplementary Information to “Phase transition and dynamics of defects in the molecular piezoelectric (TMCM)MnCl<sub>3</sub> and the effect of partial substitutions of Mn”

**Francesco Cordero, Floriana Craciun, Francesco Trequattrini, Simona Ionita, Daniel Lincu, Raul-Augustin Mitran, Victor Fruth, Simona Brajnicov, Antoniu Moldovan, Maria Dinescu**

## Materials

Trimethylamine 40% wt. aqueous solution (Sigma Aldrich, Germany), dichloromethane (Sigma Aldrich, Germany) acetonitrile (Sigma Aldrich, Germany), anhydrous MnCl<sub>2</sub> (99%, Acros Organics, Belgium) and methanol (Sigma Aldrich, Germany) were used without additional purification. NiCl<sub>2</sub>·6H<sub>2</sub>O (98%, Sigma Aldrich, Germany), CuCl<sub>2</sub>·2H<sub>2</sub>O (99%, Sigma Aldrich, Germany) and FeCl<sub>2</sub>·4H<sub>2</sub>O (99%, Sigma Aldrich, Germany) were dehydrated as presented in Sect. “Synthesis of metal-doped samples”.

## Characterization

Powder X-ray diffraction patterns were recorded using a Rigaku MiniFlex II diffractometer with Cu-K $\alpha$  radiation ( $\lambda = 1.5406 \text{ \AA}$ ). Fourier transform infrared (FT-IR) spectroscopy was performed using a Bruker Tensor 27 spectrometer. Analyses were conducted using KBr pellets, in the 4000–400 cm<sup>-1</sup> wavenumber range. Differential Scanning Calorimetry (DSC) analyses were recorded on a Mettler Toledo DSC3 calorimeter, under 200 mL·min<sup>-1</sup> nitrogen gas flow, in crimped Al pans with pierced lids. Thermogravimetric analysis (TG) and differential thermal analysis (DTA) were acquired on a Mettler Toledo TGA/SDTA851e instrument, in an oxidant environment of 80 mL·min<sup>-1</sup> synthetic air flow, using open alumina pans and 10°C·min<sup>-1</sup> heating rate.

## Synthesis of TMCM-Cl

(Chloromethyl)-trimethylammonium chloride (TMCM-Cl) was firstly synthesized starting from a 40% wt. aqueous solution of trimethylamine (0.12 mol TMA) and dichloromethane (0.15 mol), in acetonitrile (27 mL) at 40°C for 3 days [[1], [2]]. The solvent was removed under reduced pressure, using a rotary evaporator, until a dry white precipitate was formed. The resulted product is highly hygroscopic therefore it was stored under Ar gas, and further dried in a vacuum desiccator before use.

## Synthesis of TMCM-MnCl<sub>3</sub>

TMCM-Cl (5 mmol) was dissolved in methanol (10 mL) and degassed under Ar flow. The corresponding equimolar amount of anhydrous MnCl<sub>2</sub> was dissolved in methanol (10 mL) and added dropwise into the amine solution under continuous stirring. The resulting solution was slowly evaporated under a steady flow of Ar for 1 week [2]. Pale red crystals were obtained.

## Synthesis of metal-doped samples

The salts were dried before use, until the anhydrous form was obtained, as follows: NiCl<sub>2</sub>·6H<sub>2</sub>O was vacuum dried and thermally dried at 100°C, for 5 minutes, until a bright yellow powder was obtained. Anhydrous CuCl<sub>2</sub> was obtained by thermal treatment at 160°C for 48h until a brown

powder was obtained. Anhydrous  $\text{FeCl}_2$  was obtained from  $\text{FeCl}_2 \cdot 4\text{H}_2\text{O}$  in a reducing medium consisting of methanol, HCl, and metallic Fe, by evaporating the solvent under reduced pressure in a rotary evaporator, until a white powder was obtained.

The corresponding amount of each salt (0.25 mmol) was dissolved in methanol and added dropwise to a solution of  $\text{MnCl}_2$  (4.75 mmol) and TMCM-Cl (5 mmol) prepared as described before. A molar ratio of 5% metal (Ni, Cu, or Fe) to 95% Mn was used. The solutions were dried as previously specified, resulting 3 compounds: denoted as  $\text{TMCM-Mn}_{0.95}\text{M}_{0.05}\text{Cl}_3$ , where M is Ni, Cu, or Fe. Yellowish  $\text{TMCM-Mn}_{0.95}\text{Ni}_{0.05}\text{Cl}_3$  crystals, yellowish  $\text{TMCM-Mn}_{0.95}\text{Fe}_{0.05}\text{Cl}_3$  crystals, and orange  $\text{TMCM-Mn}_{0.95}\text{Cu}_{0.05}\text{Cl}_3$  crystals were obtained.

### Hygroscopicity tests

The hygroscopicity of the complex was tested by observing the aspect of the  $\text{TMCM-MnCl}_3$  in air, at an ambient temperature of 23.8 °C and a relative humidity of 33%. The perovskite was compared to the ammonium salt TMCM-Cl, which is highly hygroscopic, becoming a liquid in minutes after staying in the air. There is no visible absorption of humidity of  $\text{TMCM-MnCl}_3$ , after 120 minutes of staying in the air (Fig S1).

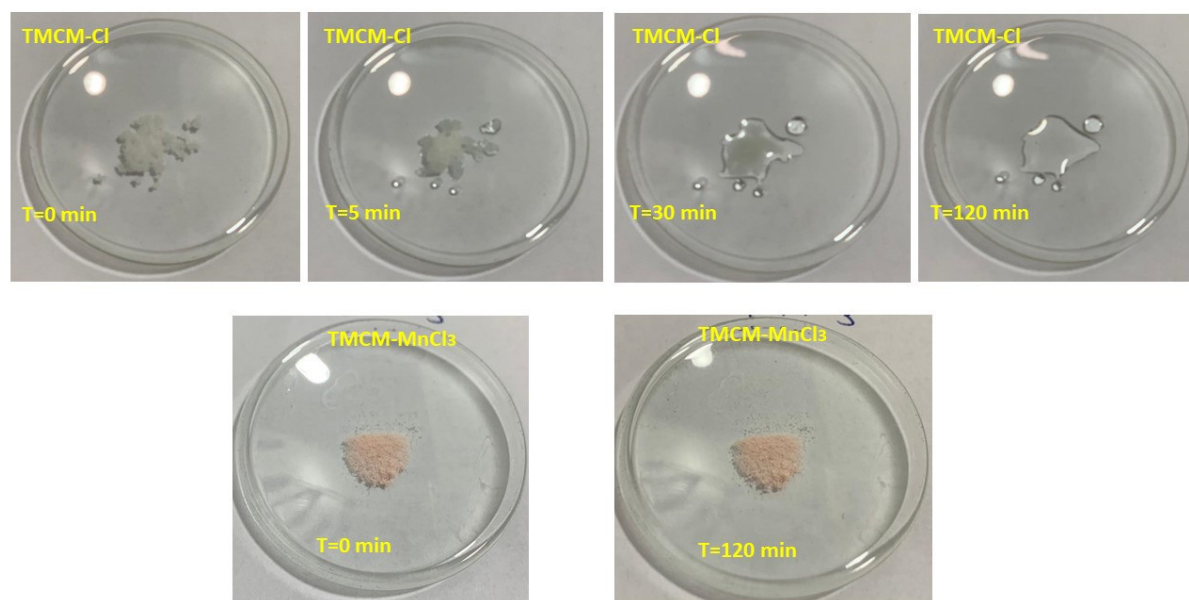


Fig. S1. Hygroscopicity observation for the ammonium salt compared to  $\text{TMCM-MnCl}_3$

### Powder XRD

The samples crystalline phases were assessed through powder X-ray diffraction (XRD) (Fig. 2 and S1 (a).) The XRD patterns of the doped samples are very similar to that reported for the  $\text{TMCM-MnCl}_3$ . For the sample containing 5% Ni the XRD pattern matches the reported simulated spectra of  $\text{TMCM-MnCl}_3$  with a *Pmma* space group [2], showing a good incorporation of the Ni in the crystal lattice. All the other samples display an additional peak at approximately  $2\theta = 16^\circ$ , which can be associated to a secondary phase as a result of inhomogeneity of the sample. A slight shift towards lower angle values is noticed when comparing 5%Fe and 5%Cu doped  $\text{TMCM-MnCl}_3$ . The shift could be explained by the changes in the interplanar distances upon doping [5].

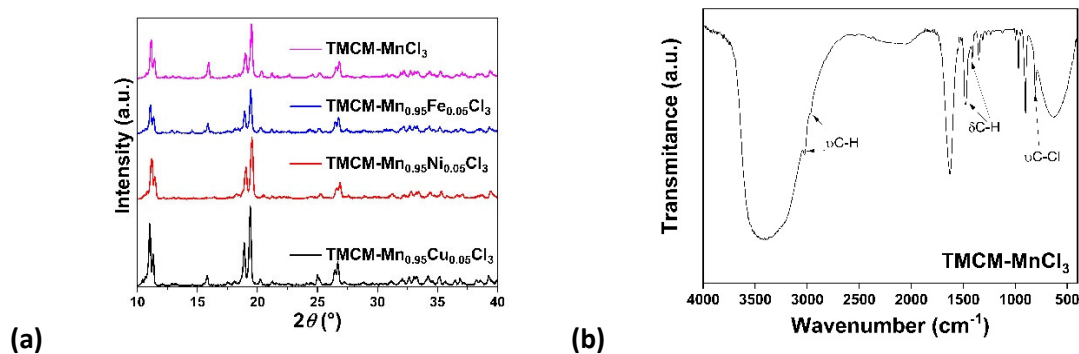


Fig. S2. (a) Powder XRD patterns for TMCM-MnCl<sub>3</sub>, TMCM-Mn<sub>0.95</sub>Fe<sub>0.05</sub>Cl<sub>3</sub>, TMCM-Mn<sub>0.95</sub>Ni<sub>0.05</sub>Cl<sub>3</sub> and TMCM-Mn<sub>0.95</sub>Cu<sub>0.05</sub>Cl<sub>3</sub>, (b) FT-IR spectrum for TMCM-MnCl<sub>3</sub> sample

### FT-IR

The FT-IR spectrum (Fig. S2 (b)) for the TMCM-MnCl<sub>3</sub> compound is in agreement with reported data, displaying the stretching vibration of the C-H bonds in CH<sub>3</sub> group at 3030 and 2960 cm<sup>-1</sup>, the deformation vibrations of these bonds at 1414 and 1485 cm<sup>-1</sup>, as well as the stretching vibration of the C-Cl bond at 806 cm<sup>-1</sup> [3,4].

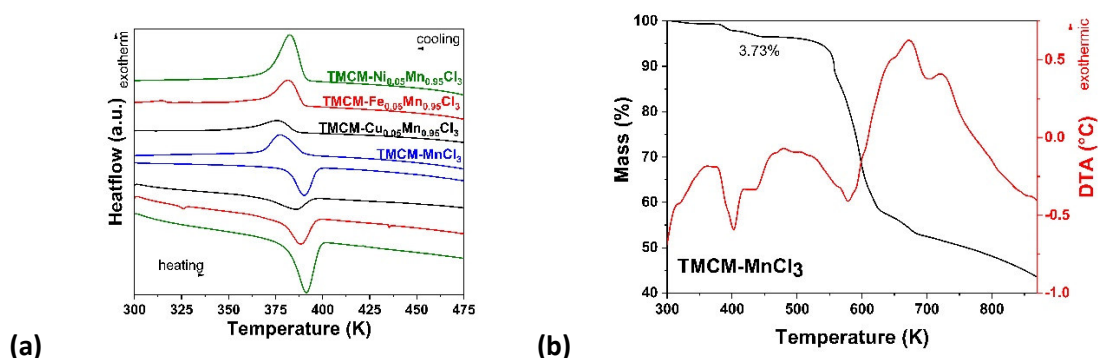


Fig. S3. (a) Heating and cooling DSC curves of TMCM-MnCl<sub>3</sub>, TMCM-Mn<sub>0.95</sub>Fe<sub>0.05</sub>Cl<sub>3</sub>, TMCM-Mn<sub>0.95</sub>Ni<sub>0.05</sub>Cl<sub>3</sub> and TMCM-Mn<sub>0.95</sub>Cu<sub>0.05</sub>Cl<sub>3</sub>, (b) Thermogravimetric (TG) and differential thermal analysis (DTA) curves for TMCM-MnCl<sub>3</sub> sample

### DSC and TGA

Differential scanning calorimetry (DSC) traces are displayed in Fig. S3a. The second heating-cooling cycle is displayed, in order to eliminate the influence of residual solvents. It seems, however, that some degradation of the materials occurred after heating the first time to high temperature, since the transition temperatures were few kelvins lower during the second thermal cycle. The transition temperatures are presented as onset temperatures. Peak temperatures were also computed for comparison with literature data. All the samples present one endothermic event upon heating, indicating one phase transition in the temperature range tested (300 – 475 K). The phase transition temperature of the TMCM-MnCl<sub>3</sub> sample is 382.1 K, being lower than that reported in the literature, 406 K [2], probably as a result of the small amount of secondary phase present in this sample, as evidenced by the XRD analyses. All the doped samples displayed phase transition temperatures similar to that of the sample TMCM-MnCl<sub>3</sub>. TMCM-Ni<sub>0.05</sub>Mn<sub>0.95</sub>Cl<sub>3</sub> sample, with the closest PXRD

pattern to that reported for TMCM-MnCl<sub>3</sub>, has a transition temperature of 381.8 K, slightly lower than that of the TMCM-MnCl<sub>3</sub> sample.

Table S1. Onset and peak temperatures of the phase transitions during the 2<sup>nd</sup> heating

| Sample   | $T_{\text{onset}}$ (K) | $T_{\text{peak}}$ (K) |
|--|------------------------|-----------------------|
| TMCM-MnCl <sub>3</sub>                                     | 382.1                  | 390.3                 |
| TMCM-Cu <sub>0.05</sub> Mn <sub>0.95</sub> Cl <sub>3</sub> | 367.8                  | 385.8                 |
| TMCM-Ni <sub>0.05</sub> Mn <sub>0.95</sub> Cl <sub>3</sub> | 381.8                  | 391.2                 |
| TMCM-Fe <sub>0.05</sub> Mn <sub>0.95</sub> Cl <sub>3</sub> | 378.4                  | 388.3                 |

The TMCM-Fe<sub>0.05</sub>Mn<sub>0.95</sub>Cl<sub>3</sub> and TMCM-Cu<sub>0.05</sub>Mn<sub>0.95</sub>Cl<sub>3</sub> samples showed a more significant decrease in the transition temperature, compared to the TMCM-MnCl<sub>3</sub> sample, with the largest difference being observed in the case of Cu-doped sample (367.8 K).

The thermogravimetric analysis of the TMCM-MnCl<sub>3</sub> sample shows a first step of ~4% mass loss below 500 K, which is associated to an endothermic event on the DTA curve, suggesting the evaporation of adsorbed humidity or solvent traces (Fig. S3b). The DTA curve also shows the phase transition event described by DSC analysis around 400 K. Starting 500 K, some endothermic and exothermic events can be observed, which are associated to the loss of the organic mass. This suggests that the compound is stable below 500 K, which is consistent with previous findings on similar compounds [6].

### Anelastic spectroscopy measurements

Figure S4a is a schematic representation of how the sample bar is mounted on thin thermocouple wires with an electrode facing the central part of the bar at close distance. For insulating sample, as in the present case, shorting of the thermocouple and counterelectrode are applied with Ag paint. An alternate voltage up to 200 V is applied to the electrode in order to excite the flexural vibration of the sample. The modulation of the capacity between the electrode and the vibrating sample is used to detect the vibration. The red arrows show that the flexural vibration causes inhomogeneous extension and compression along the sample thickness, so that the Young's modulus is probed.

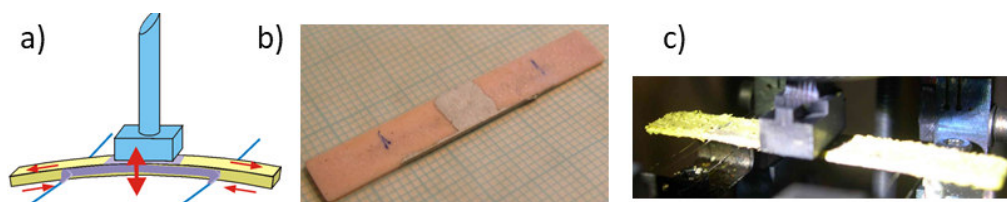


Fig. S4

A sample before being mounted in the apparatus for the anelastic measurements is shown in Fig. S4b, while Fig. S4c shows a mounted sample after being measured with intermediate openings of the vacuum system during which humidity had been absorbed: its surface is completely scaled. In some cases, the sample in this condition could be dismounted, cleaned from the scales and measured again without apparent effects on the anelastic spectrum.

## References

- [1] W. C. Davies, E. B. Evans, and F. L. Hulbert, "92. The formation of quaternary ammonium salts from dihalogenoparaffins, etc., in aqueous acetone solution," *J. Chem. Soc. (Resumed)*, no. 0, pp. 412–418, Jan. 1939, doi: 10.1039/JR9390000412.
- [2] Y. M. You *et al.*, "An organic-inorganic perovskite ferroelectric with large piezoelectric response," *Science* (1979), vol. 357, pp. 306–309, Jul. 2017, doi: 10.1126/science.aai8535.
- [3] W. Q. Liao, J. X. Gao, X. N. Hua, X. G. Chen, and Y. Lu, "Unusual two-step sequential reversible phase transitions with coexisting switchable nonlinear optical and dielectric behaviors in  $[(\text{CH}_3)_3\text{NCH}_2\text{Cl}]_2[\text{ZnCl}_4]$ ," *J. Mater. Chem. C*, vol. 5, pp. 11873–11878, 2017, doi: 10.1039/c7tc04095d.
- [4] X. N. Hua, C. R. Huang, J. X. Gao, Y. Lu, X. G. Chen, and W. Q. Liao, "High-temperature reversible phase transitions and exceptional dielectric anomalies in cobalt(ii) based ionic crystals:  $[\text{Me}_3\text{NCH}_2\text{X}]_2[\text{CoX}_4]$  (X = Cl and Br)," *Dalton Trans.*, vol. 47, pp. 6218–6224, 2018, doi: 10.1039/c8dt00786a.
- [5] S. M. Salaken, E. Farzana, and J. Podder, "Effect of Fe-doping on the structural and optical properties of ZnO thin films prepared by spray pyrolysis," *J. Semicond*, vol. 34, 073003, 2013, doi: 10.1088/1674-4926/34/7/073003.
- [6] X. N. Hua *et al.*, "A Room-Temperature Hybrid Lead Iodide Perovskite Ferroelectric," *J. Am. Chem. Soc.*, vol. 140, no. 38, pp. 12296–12302, Sep. 2018, doi: 10.1021/jacs.8b08286.